Bioorg. Med. Chem. 100 (2024) 117630

Contents lists available at ScienceDirect

Bioorganic & Medicinal Chemistry

journal homepage: www.elsevier.com/locate/bmc

Design of a novel long-acting dual GLP-1/GIP receptor agonist

Yuanzhen Dong [a,b], Jinhua Zhang [a], Hongjiang Xu [c], Hengqiao Shen [c], Qin Lu [c], Jun Feng [a,b,*], Zhengyan Cai [a,*]

[a] China State Institute of Pharmaceutical Industry, 201203 Shanghai, China
[b] Shanghai Duomirui Biotechnology Ltd, 201203 Shanghai, China
[c] Nanjing Chia Tai Tianqing Pharmaceutical Co., Ltd, Nanjing, China

ARTICLE INFO

Keywords:
GIP
GLP-1
Co-agonist
T2DM
Obesity
Long-acting potency

ABSTRACT

Tirzepatide, the first approved dual GLP-1/GIP receptor agonist (RA), has achieved better clinical outcomes than other GLP-1RAs. However, it is an imbalanced dual GIP/GLP-1 RA, and it remains unclear whether the degree of imbalance is optimal. Here, we present a novel long-acting dual GLP-1/GIP RA that exhibits better activity than tirzepatide toward GLP-1R. A candidate conjugate, D314, identified via peptide design, synthesis, conjugation, and experimentation, was evaluated using chronic studies in *db/db* and diet induced obese (DIO) mice. D314 achieved favorable blood glucose and body weight-lowering effects, equal to those of tirzepatide. Its half-life in dogs ($T_{1/2}$: 78.3 ± 14.01 h) reveals its suitability for once-weekly administration in humans. This preclinical study suggests the potential role of D314 as an effective agent for treating T2DM and obesity.

1. Introduction

Glucagon-like peptide-1 receptor agonists (GLP-1RAs) have proven successful in treating type 2 Diabetes Mellitus (T2DM), effectively reducing glucose levels, improving β-cell function, and reducing body weight.[1] Nevertheless, the development of more effective treatment methods is crucial for overcoming the ongoing difficulties many T2DM patients face in achieving their metabolic goals.[1,3] The integration of several hormone-differentiation mechanisms into individual molecules might have synergistic effects on glucose and body weight, in contrast to using a GLP-1RA alone.[4,5] An exploratory study of glucose-dependent insulin-promoting peptide (GIP), another incretin, found that it had no potential for hypoglycemic therapy.[6,7] However, new evidence suggests that using a chimeric peptide comprising amino acids from GIP and GLP-1 achieves better efficacy than using these hormones separately,[8] potentially enhancing the metabolic effects of GLP-1RA.

In May 2022, tirzepatide, the first injectable GIP/GLP-1 receptor dual agonist, was approved by the FDA for the treatment of T2DM.[9] Tirzepatide, which has a greater hypoglycemic effect than basal insulin or GLP-1RAs, led to exceptional weight loss (up to 22.5 %).[10,11] This unprecedented efficacy is consistent with the hypothesis[12] that incorporating the pharmacological properties of GIP into GLP-1 therapy will 1) improve glycemic control via dual action on pancreatic β cells, thus enhancing insulin secretion; 2) lead to GIP-driven improvements in white adipose tissue function; and 3) cause a strong anorexigenic effect by integrating the activation signals of both receptor pathways in the brain. The discovery and development of intestinal hormone co-agonists as a new class of drugs for the treatment of diabetes and obesity is a revolutionary breakthrough.[13]

Tirzepatide, a 39-amino acid synthetic peptide based on the GIP amino-acid sequence, contains a C20 unsaturated diacid acyl chain; therefore, its potency is similar to that of native GIP and ca. 20-fold lower than that of GLP-1.[12] Although tirzepatide is an imbalanced dual GIP/GLP-1 RA, it exhibits better efficacy than other GLP-1RAs; nonetheless, it remains unclear whether the degree of imbalance is completely optimal for tirzepatide.[12]

Here, we aimed to design a long-acting tirzepatide-based conjugate exhibiting high potency toward GLP-1R, while exhibiting the same potency as tirzepatide toward GIPR. A set of potent GIP and GLP-1 chimeric peptides having different activity at each receptor of interest was synthesized via solid-phase peptide synthesis (SPPS) and biochemically characterized in *vitro*. Novel albumin-binder-derived cysteine (Cys) side-chains were incorporated to prolong the half-life of the chimeric peptides.

Based on in *vitro* and in *vivo* evaluation of the conjugates, relative to tirzepatide, conjugate D314 (with a C20 diacid-γGlu-2xεLys-Lys group conjugated to the sulfhydryl group of the Cys side chain at position 20) exhibited higher potency toward GLP-1R but slightly lower potency

* Corresponding authors at: China State Institute of Pharmaceutical Industry, 201203 Shanghai, China (J. Feng).
E-mail addresses: fengjdmr@163.com (J. Feng), caizy2007@163.com (Z. Cai).

https://doi.org/10.1016/j.bmc.2024.117630
Received 17 November 2023; Received in revised form 21 January 2024; Accepted 31 January 2024
Available online 3 February 2024

toward GIPR. D314, which exhibited substantial high hypoglycemic activity and strongly induced weight loss, exhibited excellent pharmacokinetic properties following a single subcutaneous administration.

2. Results and discussion

2.1. Design and synthesis of novel GLP-1/GIP chimeric peptides

Our objective was to design a tirzepatide-based conjugate exhibiting greater potency than tirzepatide toward GLP-1R. To achieve this, we designed D01–D06, tirzepatide-based chimeric peptides with a dual GLP-1/GIP receptor agonistic effect (Fig. 1). The *N*-terminal sequences of GLP-1 (7-37) and GIP (1-42) are highly conserved and highly similar; therefore, positions 1–11 of the tirzepatide peptide sequence were used in D01–D06, with Aib residues employed at position 2 to protect against DPP-4 cleavage and inactivation. The 11 amino acids of C-terminus was from exenatide, thus enhancing peptide helicity and structural stability via intramolecular interactions.[14] Based on the structure of tirzepatide, the corresponding amino acids of GLP-1 or exenatide were introduced at residues 13, 15, 17, 19, and 21. Cys residues were introduced at residues 13, 16, 20, 21, 24, 27 to serve as anchors for subsequent modification with albumin-binding side-chains. Following the synthesis of these peptides, their potency toward GLP-1R and GIPR was tested using a cAMP assay in receptor-overexpressing CHO cells.

To varying extents, chimeric peptides D-01 to D-06 exhibited lower potency (EC_{50}) than the other compounds toward GIPR; toward GLP-1R, the chimeric peptides (except for D-04 and D-06) exhibited slightly better potency than the compounds (Table 1). In D-04, Leu at position 21 was substituted with Cys, resulting in the loss of GIPR-activity (492-fold less potent than tirzepatide) and GLP-1R activity (10-fold less potent than tirzepatide). These losses underscore the importance of amino acid 21 in GIP and GLP-1. Based on these findings, chimeric peptides D-01, D-02, D-03, and D-05, exhibiting improved GLP-1R activity but less potent activity towards the GIPR, were used for subsequent modification with fatty acids.

2.2. Design and synthesis of the conjugate

An albumin-binding side chain was attached to the peptide backbone to improve the pharmacokinetic profile of the chimeric peptides. The linker and type of fatty acid used can affect receptor pharmacology and albumin binding.[15] We therefore designed a series of novel albumin-binding reagents with long alkyl chains (C18 diacid and C20 diacid) as the albumin binders, and with AEEA-2xγGlu-Lys, γGlu-2xAEEA-Lys, and γGlu-2xεLys-Lys as hydrophilic linkers (Fig. 2A). These albumin-binding side chains exhibit excellent solubility in ethanol or saturated sodium bicarbonate, while the acetyl bromide portion of the structure enables selective attachment of the albumin-binding moiety to the Cys residue of the peptide by forming a stable thioether bond (Fig. 2B). Using this approach, conjugates D103-D114, D203-D214, D303-D314, D503-D514 were purified via reversed-phase high-performance liquid chromatography (RP-HPLC), achieving a yield of ca. 70 % (see Table 2).

Table 1
GIPR and GLP-1R potency of chimeric Cys-containing peptides and other compounds.

Peptide	EC_{50} (nM) *	
	GIPR	GLP-1R
Tirzepatide	0.030 ± 0.01	0.77 ± 0.02
GIP1-42	0.032 ± 0.01	–
Semaglutide	–	0.052 ± 0.01
D-01	0.39 ± 0.01	0.42 ± 0.02
D-02	1.87 ± 0.15	0.60 ± 0.04
D-03	0.60 ± 0.08	0.29 ± 0.05
D-04	14.78 ± 1.23	6.51 ± 1.09
D-05	2.57 ± 0.32	0.57 ± 0.11
D-06	2.33 ± 0.27	2.83 ± 0.43

* Receptor potency is expressed as the mean ± SD. All experiments were performed in triplicate and repeated three times.

2.3. In vitro activity profile

To determine whether these conjugates possess in *vitro* activity toward each receptor, we investigated their effects on cAMP production in cell lines recombinantly overexpressing GLP-1R and GIPR. Table 3 presents the potency of the conjugates with different albumin-binding side chains in stimulating human GLP-1R and GIPR: these results reveal that albumin-binding side chains that vary in terms of the type of fatty acid and hydrophilic linkers have different effects on conjugate activity; furthermore, the activity also depends on the modification site itself.

Compared with the non-derivatized forms D-01, D-02, D-03, and D-

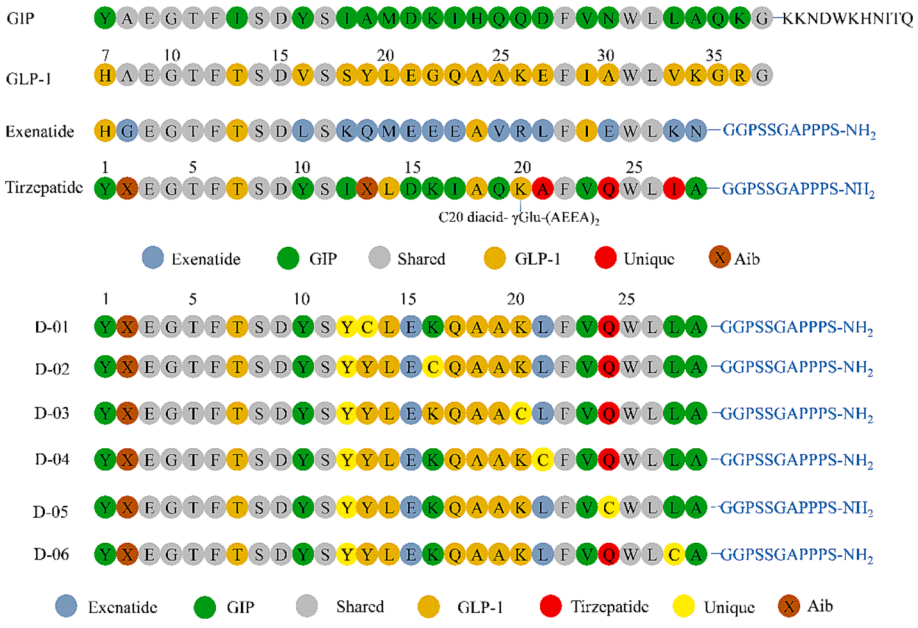

Fig. 1. Structure of GLP-1 (7-37), GIP1-42, exenatide, tirzepatide, and the novel chimeric peptides.

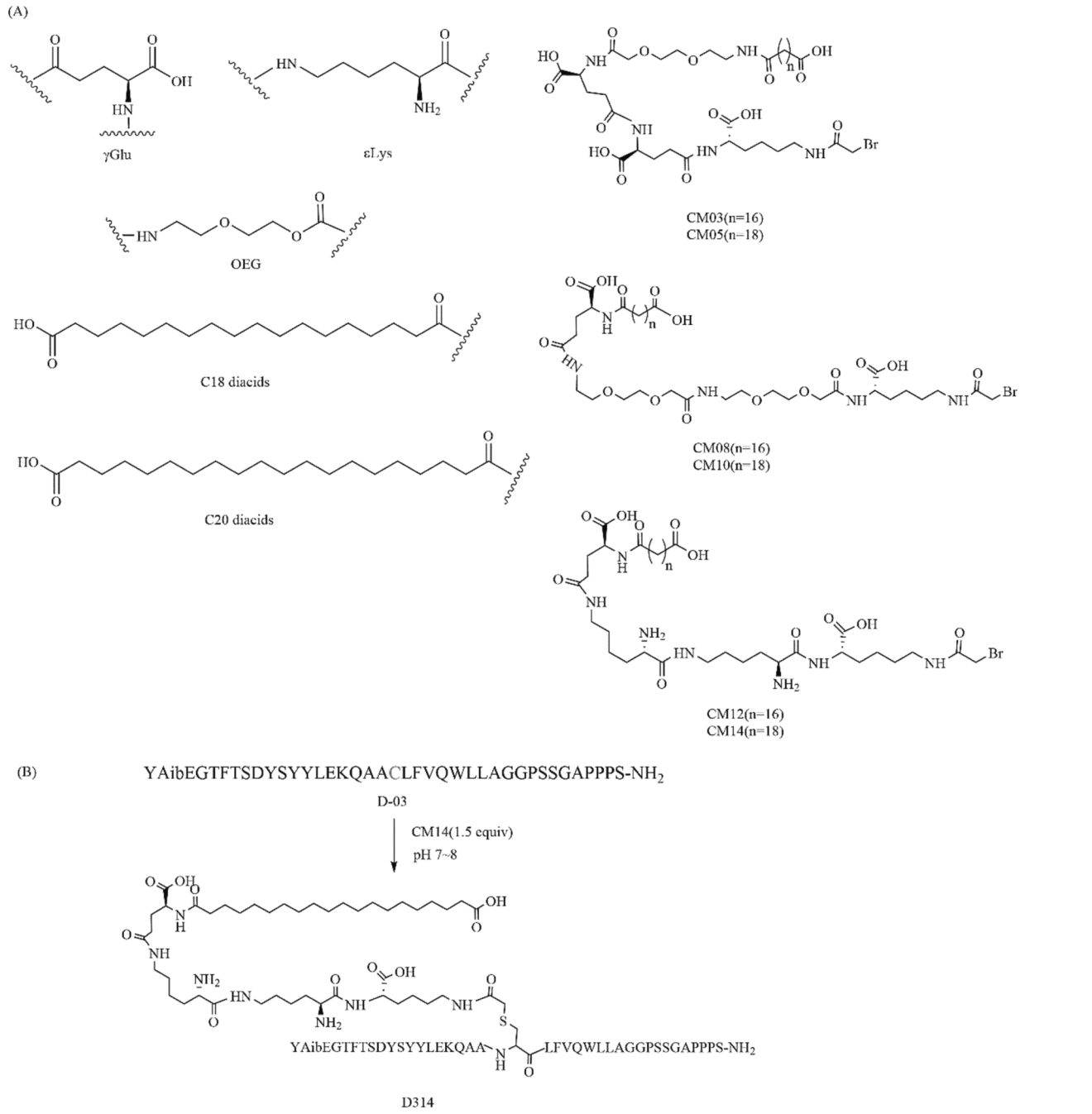

Fig. 2. (A) Structures of linkers, fatty acids, and novel albumin-binding reagents. (B) Scheme for the synthesis of D314.

05, the C18 diacid-AEEA-γGlu-γGlu-Lys analogues D103, D203, D503 and C20 diacid-AEEA-γGlu-γGlu-Lys analogues D105, 205, D505 exhibited greater GLP-1R and GIPR activity. Surprisingly, the GLP1R potency of D105 recovered from a 13-fold loss to only a 2-fold loss relative to that of tirzepatide. D303 and D305 exhibited reduced potency toward both GLP1R and GIPR.

Next, the hydrophilic linker in the side chain of AEEA-2xγGlu was substituted with γGlu-2xAEEA to generate analogs D108, D110, D310, and D510, resulting in a slight increase in the GLP1R activity of D310 and D510, while reducing the GIPR- activity of all of the conjugates.

Finally, γGlu-2xεLys-Lys, containing two amino groups, was used in the side chain to generate conjugates D114, D214, D312, D314, D512, and D514. We expected the presence of two amino groups in the side chain to increase receptor activity by the conjugates. Intriguingly, D114, D214, and D314 exhibited greater activity than the non-derivatized forms toward GIPR. In particular, D214 and D314 exhibited similar potency to tirzepatide toward GIPR (EC_{50}: 0.012 nM, 0.060 nM, and 0.030 nM, for D214, D314, and tirzepatide, respectively; Table 3) and better potency than tirzepatide toward GLP-1R. The potency lost in analog D312 was recovered by introducing the C20 diacid in D314. These results highlight the fact that differences in the hydrophilicity of linkers and fatty acid length can be designed to tune receptor activation.

The receptor activity in *vitro* of D112, D208, D210, D212, D308, and D508 toward each receptor were not measured because they exhibited poor water solubility after lyophilization.

Based on these results, conjugates D103, D105, D203, D303, D305, D114, D214, and D314 were selected for further assessment of their in vivo biological activity.

Table 2
Derivatives of D-01, D-02, D-03, D-05 with the novel Cys-linked albumin-binding reagents.

Conjugate	Peptide	Albumin-binding reagents	Purity (%)	Molecular mass			
				Calculated		Observed	
D103	D-01	CM03	95.2	5037.51	1679.4944 $[M+3H]^{3+}$	1259.8760 $[M+4H]^{4+}$	1008.5023 $[M+5H]^{5+}$
D105	D-01	CM05	96.3	5065.57	1688.8322 $[M+3H]^{3+}$	1266.8726 $[M+4H]^{4+}$	1014.0984 $[M+5H]^{5+}$
D108	D-01	CM08	97.1	5053.55	1684.8596 $[M+3H]^{3+}$	1265.3965 $[M+4H]^{4+}$	1011.7238 $[M+5H]^{5+}$
D110	D-01	CM10	96.9	5081.61	1694.5313 $[M+3H]^{3+}$	1271.1536 $[M+4H]^{4+}$	1017.3206 $[M+5H]^{5+}$
D114	D-01	CM14	95.4	5047.64	1683.5493 $[M+3H]^{3+}$	1262.4148 $[M+4H]^{4+}$	1010.3369 $[M+5H]^{5+}$
D203	D-02	CM03	95.2	5072.60	1691.8271 $[M+3H]^{3+}$	1268.6211 $[M+4H]^{4+}$	2537.2029 $[M+2H]^{2+}$
D205	D-02	CM05	96.3	5100.66	1701.1147 $[M+3H]^{3+}$	1275.5835 $[M+4H]^{4+}$	2551.1155 $[M+2H]^{2+}$
D214	D-02	CM14	96.8	5082.73	1695.2051 $[M+3H]^{3+}$	1271.6442 $[M+4H]^{4+}$	1017.5295 $[M+5H]^{5+}$
D303	D-03	CM03	95.1	5072.60	1692.1638 $[M+3H]^{3+}$	1269.8750 $[M+4H]^{4+}$	1015.4933 $[M+5H]^{5+}$
D305	D-03	CM05	99.2	5100.60	1700.8447 $[M+3H]^{3+}$	1275.6273 $[M+4H]^{4+}$	2551.2395 $[M+2H]^{2+}$
D310	D-03	CM10	97.5	5116.70	1706.5292 $[M+3H]^{3+}$	1279.8931 $[M+4H]^{4+}$	2559.2258 $[M+2H]^{2+}$
D312	D-03	CM12	98.2	5054.68	1685.5316 $[M+3H]^{3+}$	1264.1450 $[M+4H]^{4+}$	1011.9191 $[M+5H]^{5+}$
D314	D-03	CM14	96.1	5082.73	1695.2051 $[M+3H]^{3+}$	1271.6642 $[M+4H]^{4+}$	1017.5295 $[M+5H]^{5+}$
D503	D-05	CM03	96.8	5072.64	1692.5005 $[M+3H]^{3+}$	1268.6357 $[M+4H]^{4+}$	1015.5064 $[M+5H]^{5+}$
D505	D-05	CM05	95.1	5100.70	1700.8447 $[M+3H]^{3+}$	1275.6420 $[M+4H]^{4+}$	1021.1088 $[M+5H]^{5+}$
D510	D-05	CM10	98.5	5116.74	1706.2078 $[M+3H]^{3+}$	1279.6577 $[M+4H]^{4+}$	1024.3228 $[M+5H]^{5+}$
D512	D-05	CM12	96.9	5054.72	1685.8676 $[M+3H]^{3+}$	1264.4069 $[M+4H]^{4+}$	1011.5286 $[M+5H]^{5+}$
D514	D-05	CM14	96.5	5082.77	1695.2219 $[M+3H]^{3+}$	1271.6642 $[M+4H]^{4+}$	1017.3337 $[M+5H]^{5+}$

Table 3
In *vitro* activity of the conjugates.

Conjugate	Peptide	Acylation/ alkylation position	Linkage	Protractor	EC_{50} (nM) *	
					GIPR	GLP-1R
Tirzepatide	/		γGlu-2xAEEA	C20 diacid	0.030 ± 0.01	0.77 ± 0.02
D103	D-01	Cys^{13}	AEEA-2xγGlu-Lys	C18 diacid	0.14 ± 0.01	0.29 ± 0.02
D105	D-01	Cys^{13}	AEEA-2xγGlu-Lys	C20 diacid	0.064 ± 0.013	0.25 ± 0.03
D108	D-01	Cys^{13}	γGlu-2xAEEA-Lys	C18 diacid	1.31 ± 0.35	1.75 ± 0.12
D110	D-01	Cys^{13}	γGlu-2xAEEA-Lys	C20 diacid	0.42 ± 0.13	1.34 ± 0.54
D114	D-01	Cys^{13}	γGlu-2xAEEA-Lys	C20 diacid	0.14 ± 0.01	0.46 ± 0.05
D203	D-02	Cys^{16}	AEEA-2xγGlu-Lys	C18 diacid	0.11 ± 0.01	0.14 ± 0.02
D205	D-02	Cys^{16}	AEEA-2xγGlu-Lys	C20 diacid	0.20 ± 0.11	0.51 ± 0.13
D214	D-02	Cys^{16}	γGlu-2xAEEA-Lys	C20 diacid	0.012 ± 0.011	0.52 ± 0.23
D303	D-03	Cys^{20}	AEEA-2xγGlu-Lys	C18 diacid	0.67 ± 0.14	1.02 ± 0.25
D305	D-03	Cys^{20}	AEEA-2xγGlu-Lys	C20 diacid	0.73 ± 0.34	1.25 ± 0.12
D310	D-03	Cys^{20}	γGlu-2xAEEA-Lys	C20 diacid	1.31 ± 0.26	0.49 ± 0.01
D312	D-03	Cys^{20}	γGlu-2xεLys-Lys	C18 diacid	19.19 ± 2.12	1.26 ± 0.45
D314	D-03	Cys^{20}	γGlu-2xεLys-Lys	C20 diacid	0.06 ± 0.01	0.18 ± 0.02
D503	D-05	Cys^{24}	AEEA-2xγGlu-Lys	C18 diacid	0.46 ± 0.11	0.29 ± 0.13
D505	D-05	Cys^{24}	AEEA-2xγGlu-Lys	C20 diacid	1.12 ± 0.21	0.44 ± 0.02
D510	D-05	Cys^{24}	γGlu-2xAEEA-Lys	C20 diacid	3.73 ± 0.78	0.89 ± 0.04
D512	D-05	Cys^{24}	γGlu-2xεLys-Lys	C18 diacid	2.76 ± 0.32	0.40 ± 0.02
D514	D-05	Cys^{24}	γGlu-2xεLys-Lys	C20 diacid	7.2 ± 1.1	0.29 ± 0.01

*Receptor potency is expressed as the mean ± SD. All experiments were performed in triplicate and repeated three times.

2.4. Biological activity in normal (ICR) mice

Using ICR mice, an oral glucose tolerance test was performed after replacing the glucose with corn starch. Following corn-starch gavage, mice administered saline exhibited a marked increase in blood glucose levels, whereas those administered conjugates D105, D203, D303, D305, D505, D214, and D314 exhibited less pronounced increases (Fig. 3A, B). Relative to the saline control, $AUC_{(0\text{-}72h)}$ differed significantly for all of the conjugates except D114.

The conjugates did not all result in sustained weight loss (Fig. 3c). Most of the compounds led to weight loss one day after administration, while mice administered D103 and D203 started to gain weight on day 2

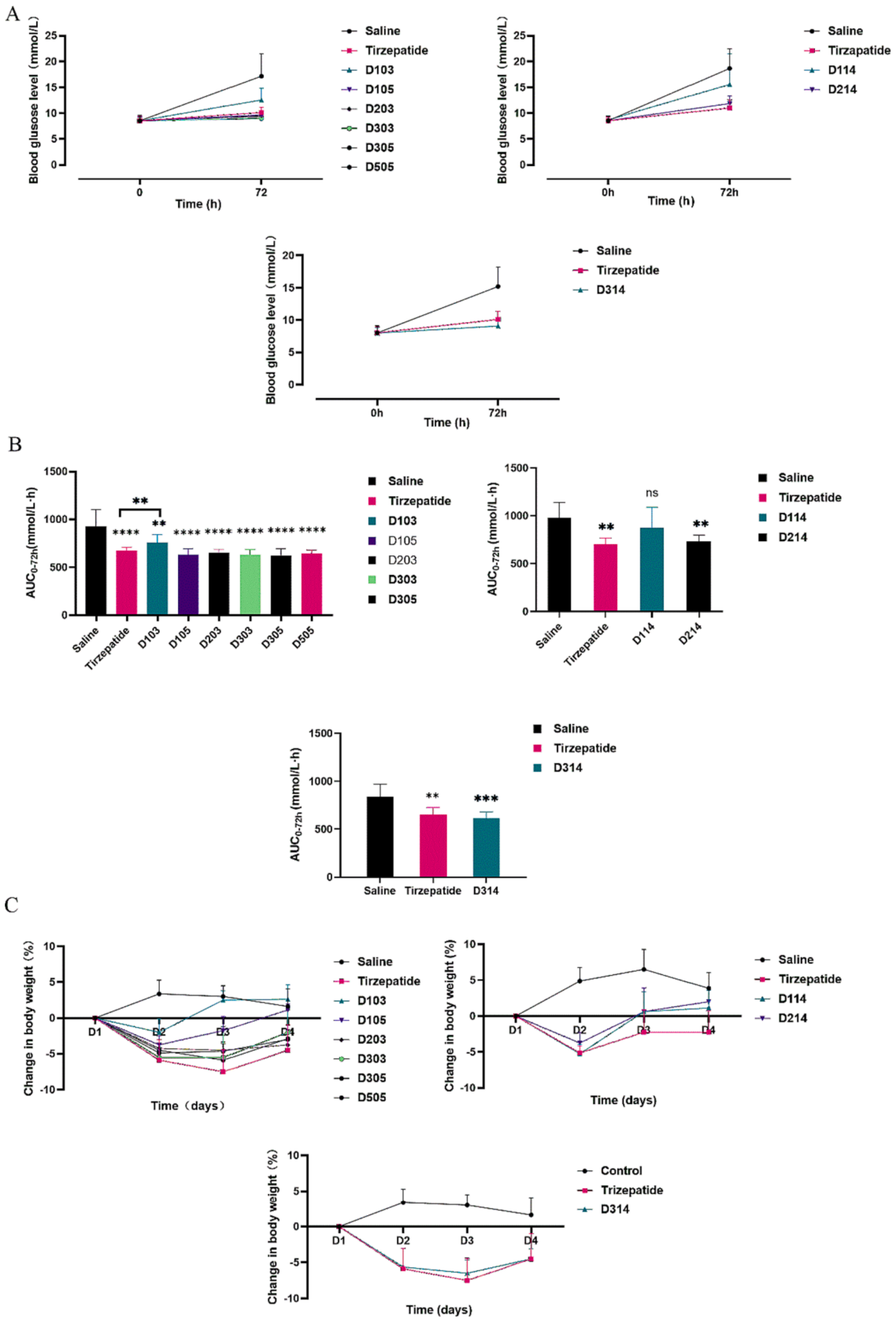

Fig. 3. Biological activity in normal (ICR) mice. (A) Glucose-lowering effects; (B) Calculated plasma glucose $AUC_{0\text{-}72h}$; (C) Change in body weight. Data are given as the mean ± SD, n = 8. Differences were determined using one-way ANOVA followed by Dunnett's test to compare treatment effects versus the vehicle control group. $^{*}p < 0.05$, $^{**}p < 0.01$, $^{***}p < 0.001$, $^{****}p < 0.0001$ versus vehicle control group.

after administration. D314 had a similar effect on weight loss as tirzepatide, causing a significantly greater reduction in body weight than the saline control.

Based on these promising in *vitro* and in *vivo* results, D314 was chosen for further assessment of its in *vivo* biological activities in *db/db* and diet induced obese (DIO) mice.

2.5. In vivo chronic study of D314 in DIO mice

The effects of D314 on body weight were characterized in a diet-induced obesity (DIO) mouse model. Mice in the model group were subcutaneously administered phosphate-buffered saline (PBS), semaglutide (30 nmol/kg), tirzepatide (10 nmol/kg), or D314 (10 nmol/kg) every 3 days for 46 days. Significant weight loss was observed following treatment with D314, tirzepatide, and semaglutide ($p < 0.05$, Fig. 4A, B). The vehicle-treated control group exhibited a body weight change of +4 % on day 46, whereas D314, tirzepatide and semaglutide resulted in changes of −21 %, −21 %, −10 %, respectively on day 46.

2.6. In vivo chronic study of D314 in db/db mice

Db/db male mice were used for chronic (long-term) exposure testing by subcutaneous administrating PBS, semaglutide, tirzepatide, or conjugate D314 (30 nmol/kg) every 3 days for 60 days. Blood glucose levels were measured 72 h after administration. Up to day 31, D314 appeared to have a more potent hypoglycemic effect than semaglutide, similar to that of tirzepatide, whereas in the later stages of administration, the effect of D314 on blood glucose varied significantly (Fig. 5A).

D314 and tirzepatide both exhibited good weight-reducing effects in *db/db* mice, with D314 having the stronger effect (Fig. 5B). Body weight increased slightly in the semaglutide group. The weight loss observed in the vehicle group may be related to sustained hyperglycemia.

Relative to the saline treatment, HbA_{1c} levels were significantly lower following the other treatments; in the D314 and semaglutide groups, HbA_{1c} initially decreased and then remained unchanged, while in the tirzepatide group it exhibited a slight but continuous decrease (Fig. 5C).

GLP-1/GIP agonists result in body weight reduction by inhibiting food intake.[8] Food intake was recorded every 3 days. D314 at 30 nmol/kg achieved a greater reduction in food intake than semaglutide or tirzepatide at the same dose (Fig. 5D).

2.7. In vivo pharmacokinetics

Pharmacokinetics were examined in Beagle dogs to determine the half-life of D314. D314 was absorbed into the plasma after single subcutaneous administration: its T_{max} ranged from 8 to 24 h, elimination half-life from 63.9 to 80.1 h, and its maximum plasma concentration was 215 ng/mL (Table 4). Tirzepatide reached a maximum plasma concentration of 344 ng/mL in ca. 8–24 h. D314 absorption was slightly slower than tirzepatide absorption; the D314 exposure level was ca. 0.675 times lower than that of tirzepatide; and D314 was eliminated ca. 0.835 times faster than tirzepatide (Fig. 6).

Acylation to promote albumin binding is one of the most effective ways to extending the in *vivo* half-life of therapeutic peptides.[15] Peptide pharmacokinetic properties depend strongly on the position of the fatty acid and linker in the backbone and on the type of fatty acid and linker.[16,17] In tirzepatide, the C20 diacid is conjugated to the ε-amino group of Lys at position 20 ia the 2xAEEA spacer and a γ-Glu linker; and in BI456906, a C-18 fatty diacid is linked via a glycine-serine spacer,[18] enabling a once-weekly dosing frequency in humans.[19] D314 has a C20 diacid linked by γGlu-2xεLys-Lys spacer, and the albumin-binding moiety forms a thioether bond to the modified Cys residue at position 20. Based on the pharmacokinetic properties of D314, derivatization of the Cys residue thiol group can achieve promising pharmacokinetic profiles in *vivo*.

3. Conclusions

Several multi-receptor agonists have entered clinical trials for the treatment of patients with T2D obesity or nonalcoholic steatohepatitis (NASH) and have been tested against selective GLP-1Ras.[20] In multiple head-to-head clinical trials, tirzepatide has exhibited profound therapeutic superiority in reducing body weight and blood glucose relative to several drugs on the market, including semaglutide[10] and dulaglutide.[11]

The aim of this study was to design a long-acting co-agonist candidate with higher GLP-1R potency than tirzepatide, while maintaining the same GIPR potency as tirzepatide. Instead of a Lys residue, we used a Cys residue as an anchor for subsequent modification with albumin-binding side chains. Mutation of tirzepatide's Aib at position 13 to Tyr made it possible to prepare the peptide via fermentation, which is environmentally safer and cheaper than other methods. Almost all of the chimeric peptides developed exhibited reduced GIPR activity and improved GIP-1R activity, whereas GIPR potency was recovered for conjugates D105, D214, and D314. This highlights the impact of fatty acids and differences in linker hydrophilicity on pharmacological properties, and reveals that fatty acid length can be adjusted to tune receptor activation.

Finally, using DIO mice, the anti-obesity effects of D314 were compared with those of tirzepatide and semaglutide. D314 achieved similar weight loss to the selective GIP/GLP-1 receptor co-agonist tirzepatide and significantly greater weight loss than the GLP-1 receptor

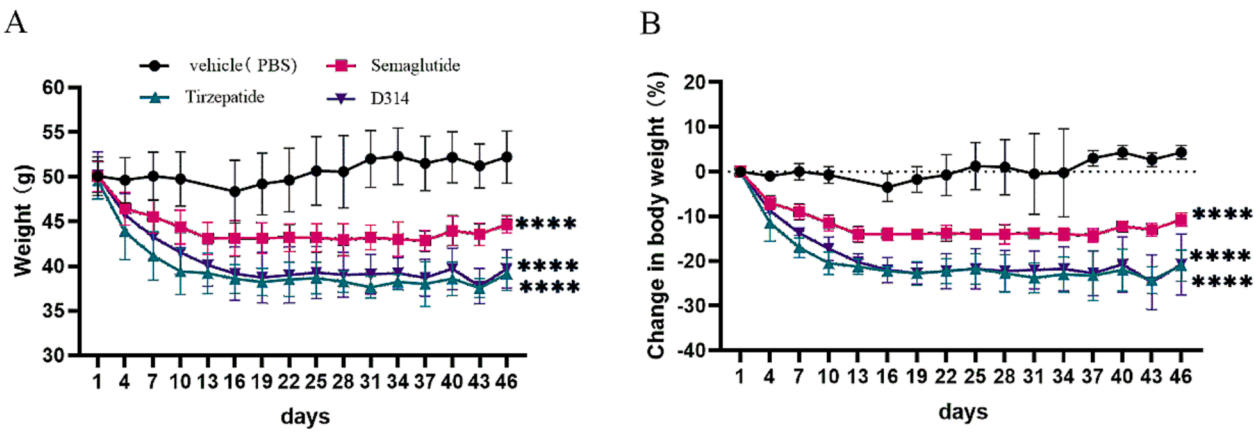

Fig. 4. The anti-obesity activity of D314 in diet-induced obese (DIO) mice. (A) Overall body weight and (B) Body weight change. Data are given as the mean ± SD, n = 4 Differences were determined using one-way ANOVA followed by Dunnett's test to compare treatment effects versus vehicle control group. *$p < 0.05$, **$p < 0.01$, ***$p < 0.001$, ****$p < 0.0001$ versus vehicle control group.

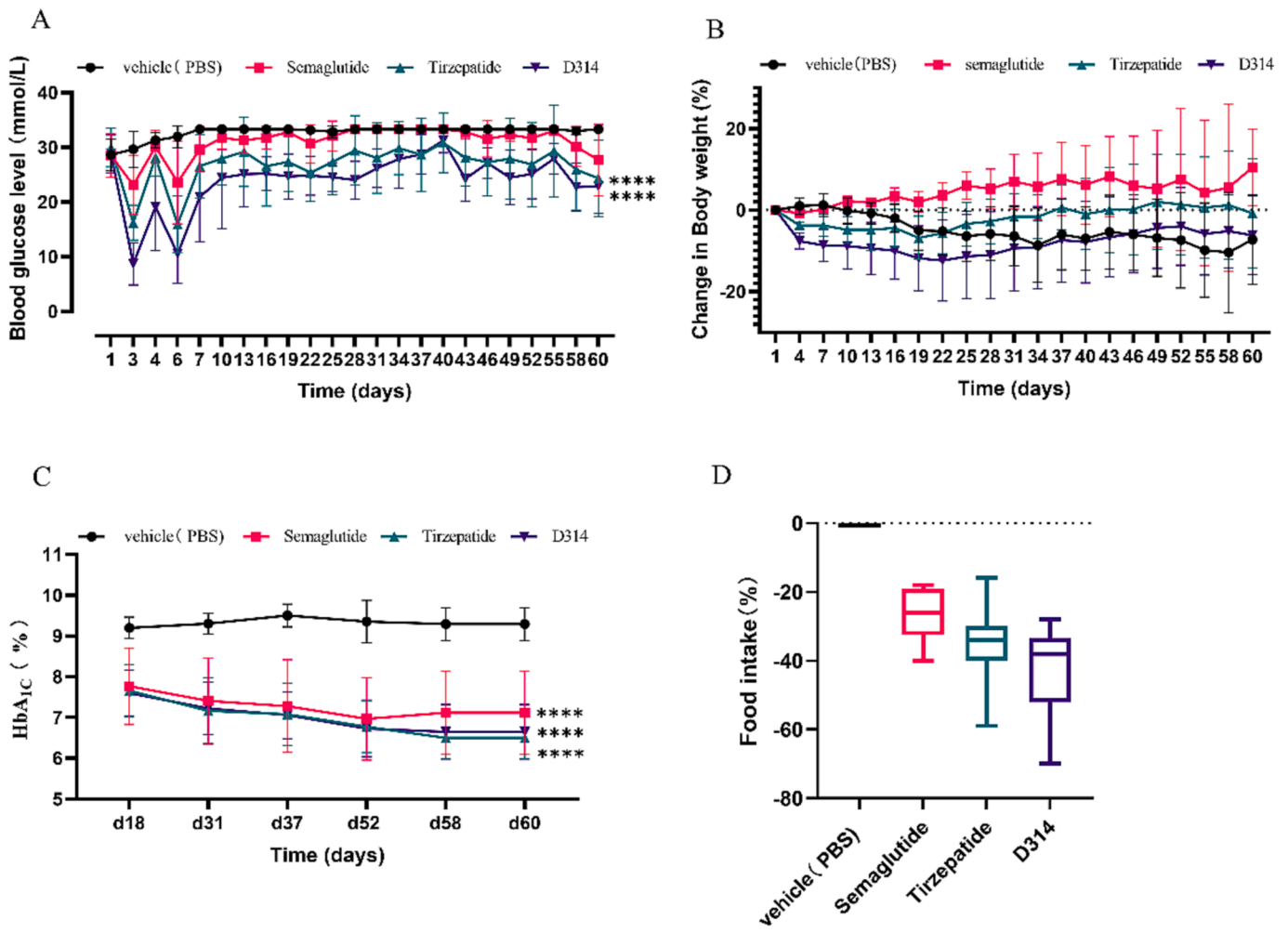

Fig. 5. Effects of D314 in *db/db* mice. (A) Blood glucose level, (B) Body weight change, (C) Change in HbA1c, and (D) Cumulative food intake of *db/db* mice treated with vehicle, semaglutide, tirzepatide, or D314. Data are given as the mean ± SD, n = 5. Differences were determined using one-way ANOVA followed by Dunnett's test to compare treatment effects versus vehicle control group. $p < 0.05$ was considered statistically significant. *$p < 0.05$, **$p < 0.01$, ***$p < 0.001$, ****$p < 0.0001$ versus vehicle control group.

Table 4
Pharmacokinetic parameters of D314 and tirzepatide in Beagle dogs following a single subcutaneous administration.

	Tirzepatide	D314
T_{max} (h) (Mean ± SD)	14 ± 8.72	18.7 ± 9.25
C_{max} (ng/mL) (Mean ± SD)	344 ± 10	215 ± 37.6
$AUC_{0\text{-}168h}$ (h × ng/mL) (Mean ± SD)	35123 ± 2162	23720 ± 2664
$t_{1/2}$ (h) (Mean ± SD)	93.8 ± 8.61	78.3 ± 14.01

mono-agonist semaglutide. In diabetic *db/db* mice, chronic D314 dosing significantly reduced blood glucose and reduced food consumption. These reductions were correlated with a reduction in body weight to the same extent as for tirzepatide. D314 exhibited comparable pharmacokinetic properties to tirzepatide, making it suitable for once-weekly administration in humans.

In summary, conjugate D314, with its promising pharmacological and pharmacokinetic profile, is suitable for the treatment of diabetes and obesity. In future studies, we will examine the receptor-binding affinity and pharmacodynamics of D314 in a DIO mouse model and *db/db* mice, considering the effect of dose.

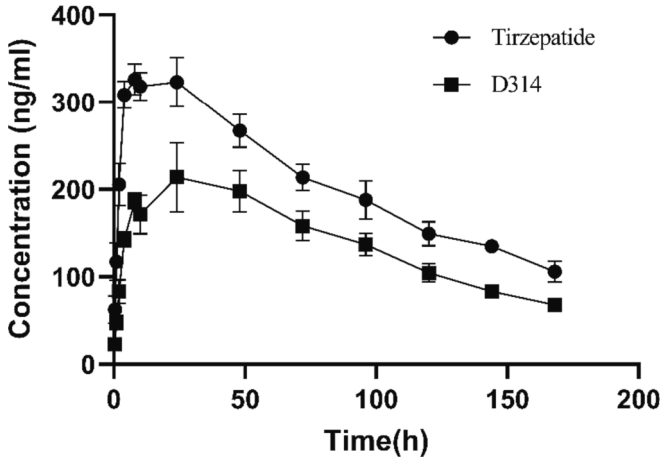

Fig. 6. Average plasma concentrations of D314 and tirzepatide in Beagle dogs (n = 3), after single subcutaneous injection at 10 nmol/kg.

4. Materials and methods

4.1. Materials

Fmoc-protected amino acids were purchased from CSBio (China); Rink Amide MBHA resin and Fmoc-Lys (Alloc)-Wang resin from Sunresin New Materials Co., Ltd. (China); N, *N*-dimethylformamide and dichloromethane from Shanghai Suyuan Chemical Co., Ltd. (China); HOBt and DIC from Aladdin (China). Trifluoroacetic acid (TFA) and triisopropylsilane (TIS) from Macklin (Shanghai, China); tirzepatide from Guotai Biotechnology Co. Ltd. (China); LANCE UltracAMP Kit from Perkin Elmer (Milford, MA); GLP-1R-CRE-bla CHO-K1 cells from Life Technologies Corporation (Carlsbad, CA); and the cAMP Hunter CHO-K1GIPR Gs Cell Line from Eurofins DiscoverX (Fremont, CA, USA).

4.2. Animals

ICR mice (male, age 10 weeks, 30–35 g) were purchased from Shanghai Lingchang Biological Technology (China); *Db/db* mice (male, 26 weeks old,45–55 g) from Jiangsu Jicui Yaokang Biotechnology (China); and DIO mice (male, 45–55 g) from Shanghai Model Organisms Center, Inc. The animal experiments were conducted according to the Laboratory Animal Management Regulations of China and adhered to the Guide for the Care and Use of Laboratory Animals published by the National Institutes of Health (2011). The experiments were conducted to minimize the number of animals used and their suffering. The reagents were of analytical or equivalent grade. Double-distilled water was used in all the experiments.

4.3. Chimeric peptide synthesis and purification

The C-terminally amidated GLP-1/GIP chimeric peptides were synthesized by SPPS on Rink MBHA Amide resin using Fmoc-protected amino acid in an Automated Microwave Peptide Synthesizer (Biotage Initiator+ Alstra, Sweden). Peptides were cleaved from the resin and deprotected by treatment with TFA containing 2.5 % TIS, 2.5 % H_2O. The peptide was precipitated with cold ethyl ether from a filtered TFA solution according to the standard procedure.[21] Peptides were purified by preparative reverse-phase HPLC on a C4 column (30 nm, 10 × 250 mm, 10 μm) with gradient elution (Phase A: 0.05 mol/L potassium hydrogen phosphate anhydrous [K_2HPO_4], 2.5 mmol/L Tris (β-chloroethyl) phosphate [TCEP], pH 8.0; Phase B: Acetonitrile). All peptides were 90 % pure as determined by analytical HPLC. The purified peptides were characterized via liquid chromatography–mass spectrometry (LC–MS) (UPLC-Xevo G2-XS QTOF, Waters Corp., Milford, MA, USA).

4.4. Conjugation

The albumin-binding side-chain was assembled on an Fmoc-Lys (Alloc)-Wang resin using standard Fmoc solid-phase synthesis. The reactions were conducted by incubating 5 mg of chimeric peptide with 1.5 equiv of side-chain in 1 mL of PBS at pH 7–8. The mixture was stirred at room temperature for 15–30 min, and the reaction progress was monitored using analytical high-performance liquid chromatography (HPLC). After > 95 % of the peptide was consumed, the product was directly purified by preparative HPLC. The final products were identified via LC–MS.

4.5. Human GLP-1, GIPreceptor activation

The pharmacological activity of each analog was determined in CHO cells stably expressing the human GLP-1 receptor (GLP-1R), gastric inhibitory peptide receptor (GIPR) using a cell-based assay that measures cAMP production, as previously reported.[22] Cells were grown in Dulbecco's modified Eagle's medium (DMEM) with the addition of 25 mmol/L HEPES, 0.1 mmol/L non-essential amino acids, 100 μg/mL penicillin, 100 μg/mL streptomycin, and 10 % (v/v) fetal bovine serum (FBS) at 37 °C in 5 % CO_2. Before the test, approximately 1000 cells per well were seeded in 384-well solid black microplates. Test conjugates diluted in DMEM and 1 % (v/v) FBS were added to the corresponding wells, and the mixture was incubated for 30 min. After the first incubation, 5 μL Eu-cAMP tracer working solution and 5 μL ULight-anti-cAMP work solution were added to each well, followed by incubation for another 60 min. The 384-well plate was then transferred to a SpectraMax i3x Multi-Mode Microplate Reader (Molecular Devices, San Jose, CA) for HTRF detection at 665/620 nm.

4.6. Glucose tolerance tests

An in *vivo* biological activity assay was performed using normal (ICR) mice, as previously described[22]. Male ICR mice (32–38 g) were individually housed in a temperature-controlled (20–26 ℃) facility with a 12 h light/dark cycle and free access to food and water. They were randomly divided into groups of 8 animals per group. After measuring the baseline blood glucose, the mice were fasted for 2 h, and peptides were subcutaneously administered at 30 nmol/kg; 71 h after administration, the mice were administered cornstarch solution (10.6 g/kg) by gavage as a challenge, and tail blood glucose was measured 60 min later.

4.7. In vivo chronic study of D314 in DIO mice

DIO male C57/B16 mice (26 weeks old, 45–55 g) were used. Animals were individually housed in a temperature-controlled (20–26 °C) facility with a 12 h light/dark cycle and free access to food and water. The mice were randomized into treatment groups (n = 4) based on body weight and basic blood glucose levels. Mice in the model group were subcutaneously administered PBS, semaglutide (30 nmol/kg), tirzepatide (10 nmol/kg), or D314 (10 nmol/kg) every three days for 46 days. Body weight was recorded every 3 days.

4.8. In vivo chronic study of D314 in db/db mice

Male *db/db* mice (45–55 g) were used. Animals were individually housed in a temperature-controlled (20–26 °C) facility with a 12 h light/dark cycle and free access to food and water. The mice were randomized into treatment groups (n = 5 per group) based on body weight and baseline blood glucose levels. The mice in the model group were subcutaneously administered PBS, semaglutide, tirzepatide, or their conjugates (30 nmol/kg) every 3 days for 60 days. Body weight and food intake were recorded every 3 days. Blood glucose levels were measured 72 h after each administration. Orbital blood samples (ca. 60 μL; 15 % EDTA was added as an anticoagulant) were taken, and HbA_{1c} was determined using an Auto-Chemistry Analyzer (CS-1200, China), at 18, 31, 37, 52, 58 and 60 days.

4.9. In vivo pharmacokinetic analysis

Beagle dogs weighing 10–13 kg were randomized into treatment groups (n = 3 per group). Whole blood samples (1 mL) were collected from a subcutaneous forelimb vein in pre-chilled K_2 EDTA tubes at 0 min and 3, 6, 10, 24, 48, 72, 96, 120, 144, and 168 h after administration of PBS, semaglutide, tirzepatide, or their conjugates (10 nmol/kg) via a single subcutaneous dose. The plasma was separated by centrifugation at 4000 rpm and 4 °C for 10 min. The plasma was then added to a low adsorption centrifuge tube and stored at −80 °C. After thawing, 100 μL plasma was transferred to a 1.5 mL centrifuge tube and 50 μL internal standard solution was added at 1 μg/mL. This was supplemented with 150 μL acetonitrile: methanol mixture at 3:2 (0.1 % glacial acetic acid), vortexed for 3 min, centrifuged for 10 min (18,000*g* at 4 °C); 200 μL of the supernatant was then transferred to a 2.2 mL low-adsorption 96-well plate for LC–MS/MS (injection volume 1 μL). The pharmacokinetic parameters and half-lives were calculated using WinNonlin v. 8.2 using a

noncompartmental model.

4.10. Data analysis and statistical significance

The data were analyzed using GraphPad Prism v. 9.5. Effects were tested using one-way ANOVA followed by Dunnett's test for pairwise comparisons. Data are presented as the mean ± standard deviation (SD).

CRediT authorship contribution statement

Yuanzhen Dong: Writing – review & editing, Writing – original draft, Visualization. **Jinhua Zhang:** Writing – review & editing, Visualization. **Hongjiang Xu:** Supervision. **Hengqiao Shen:** Validation. **Qin Lu:** Validation. **Jun Feng:** Project administration. **Zhengyan Cai:** Project administration.

Declaration of competing interest

The authors declare that they have no known competing financial interests or personal relationships that could have appeared to influence the work reported in this paper.

Data availability

Data will be made available on request.

Acknowledgements

The authors thank Nanjing Chia Tai Tianqing Pharmaceutical Co., Ltd., and Shanghai Duomirui Biotechnology Ltd. This study received no specific grants from funding agencies in the public, commercial, or not-for-profit sectors.

Appendix A. Supplementary data

Supplementary data to this article can be found online at https://doi.org/10.1016/j.bmc.2024.117630.

References

1. Nauck MA, Quast DR, Wefers J, et al. GLP-1 receptor agonists in the treatment of type 2 diabetes–state-of-the-art. *Mol Metabol*. 2021;46, 101102.
2. Min T, Bain SC. The role of tirzepatide, dual GIP and GLP-1 receptor agonist, in the management of type 2 diabetes: the SURPASS clinical trials. *Diabetes Therapy*. 2021;12:143–157.
3. Aroda VR, Ahmann A, Cariou B, et al. Comparative efficacy, safety, and cardiovascular outcomes with once-weekly subcutaneous semaglutide in the treatment of type 2 diabetes: insights from the SUSTAIN 1–7 trials. *Diabetes Metab*. 2019;45:409–418.
4. Tschöp MH, Finan B, Clemmensen C, et al. Unimolecular polypharmacy for treatment of diabetes and obesity. *Cell Metab*. 2016;24:51–62.
5. Day JW, Ottaway N, Patterson JT, et al. A new glucagon and GLP-1 co-agonist eliminates obesity in rodents. *Nat Chem Biol*. 2009;5:749–757.
6. Bastin M, Andreelli F. Dual GIP–GLP1-receptor agonists in the treatment of type 2 diabetes: a short review on emerging data and therapeutic potential. *Diabetes, Metabolic Syndrome Obesity*. 2019;12:1973–1985.
7. Vilsbøll T, Knop FK, Krarup T, et al. The pathophysiology of diabetes involves a defective amplification of the late-phase insulin response to glucose by glucose-dependent insulinotropic polypeptide—regardless of etiology and phenotype. *J Clin Endocrinol Metab*. 2003;88:4897–4903.
8. Finan B, Ma T, Ottaway N, et al. Unimolecular dual incretins maximize metabolic benefits in rodents, monkeys, and humans. *Sci Transl Med*. 2013;5:209ra151.
9. Mullard A. Lilly's tirzepatide secures first approval in diabetes, paving path for dual-acting hormone mimetics. *Nat Rev Drug Discov*. 2022;21:480.
10. Del Prato S, Kahn SE, Pavo I, et al. Tirzepatide versus insulin glargine in type 2 diabetes and increased cardiovascular risk (SURPASS-4): a randomised, open-label, parallel-group, multicentre, phase 3 trial. *Lancet*. 2021;398:1811–1824.
11. Inagaki N, Takeuchi M, Oura T, Imaoka T, Seino Y. Efficacy and safety of tirzepatide monotherapy compared with dulaglutide in Japanese patients with type 2 diabetes (SURPASS J-mono): a double-blind, multicentre, randomised, phase 3 trial. *Lancet Diabetes Endocrinol*. 2022;10:623–633.
12. Willard FS, Douros JD, Gabe MBN, et al. Tirzepatide is an imbalanced and biased dual GIP and GLP-1 receptor agonist. *JCI Insight*. 2020;5:e140532.
13. Nogueiras R, Nauck MA, Tschöp MH. Gut hormone co-agonists for the treatment of obesity: from bench to bedside. *Nat Metab*. 2023;5:933–944.
14. Elvers A, Haack T, Lorenz M, et al. Design of novel exendin-based dual glucagon-like peptide 1 (GLP-1)/glucagon receptor agonists. *J Med Chem*. 2017;60:4293–4303.
15. Kurtzhals P, Østergaard S, Nishimura E, Kjeldsen T. Derivatization with fatty acids in peptide and protein drug discovery. *Nat Rev Drug Discov*. 2023;22:59–80.
16. Lau J, Bloch P, Schäffer L, et al. Discovery of the once-weekly glucagon-like peptide-1 (GLP-1) analogue semaglutide. *J Med Chem*. 2015;58:7370–7380.
17. Østergaard S, Paulsson JF, Kofoed J, et al. The effect of fatty diacid acylation of human PYY3-36 on Y2 receptor potency and half-life in minipigs. *Sci Rep*. 2021;11:21179.
18. Zimmermann T, Thomas L, Baader-Pagler T, et al. BI 456906: Discovery and preclinical pharmacology of a novel GCGR/GLP-1R dual agonist with robust anti-obesity efficacy. *Mol Metab*. 2022;66, 101633.
19. Yazawa R, Ishida M, Balavarca Y, et al. A randomized Phase I study of the safety, tolerability, pharmacokinetics and pharmacodynamics of BI 456906, a dual glucagon receptor/glucagon-like peptide-1 receptor agonist, in healthy Japanese men with overweight/obesity. *Diabetes Obes Metab*. 2023;25:1973–1984.
20. Campbell JE, Müller TD, Finan B, et al. GIPR/GLP-1R dual agonist therapies for diabetes and weight loss—chemistry, physiology, and clinical applications. *Cell Metab*. 2023;35:1519–1529.
21. Li Y, Dong Y, Lu J, et al. Design, synthesis and antibacterial activity of novel colistin derivatives with thioether bond-mediated cyclic scaffold. *J Antibiotics: Int J*. 2023;76:260–269.
22. Zhang J, Dong Y, Ju D, Feng J. Design, synthesis and biological evaluation of double fatty chain-modified glucagon-like peptide-1 conjugates. *Bioorg Med Chem*. 2021;44, 116291.